

Liquid ^4He on Cs: drying, depinning, and the non-wetting ‘thin-film’

D Reinelt, V Iov, P Leiderer and J Klier¹

Department of Physics, University of Konstanz, D-78457 Konstanz, Germany

E-mail: juergen.klier@uni-konstanz.de

Received 24 November 2004

Published 18 February 2005

Online at stacks.iop.org/JPhysCM/17/S403

Abstract

Liquid ^4He shows a dewetting phase on Cs and Rb at low temperatures. These are the only substrates which are not wetted by ^4He . On Cs the wetting temperature, T_w , is about 2 K. Usually one observes a thick metastable helium film remaining on the Cs substrate when either the surface is cooled below T_w (so starting from a wet film) or when bulk helium (in the form of a drop or an advancing film) is deposited on the Cs. The contact line of this film is generally very stable and so there is no dewetting. However, we have observed that spontaneous drying of helium on Cs can occur and that contact lines can recede for temperatures close to T_w . This exceptional behaviour is analysed and the dependence of substrate roughness is discussed. Furthermore, we have studied the non-wetting ‘thin-film’ of liquid ^4He on Cs. Far away from coexistence this film grows as a two-dimensional (2D) gas until about one monolayer is obtained, then remains nearly constant for a certain range of chemical potential and, close to coexistence, rapidly forms a thicker 2D-liquid-like film as stable thermodynamical solution.

1. Introduction

The surfaces of alkali metals are weak-binding substrates for ^4He atoms. This was theoretically demonstrated and a non-wetted state for liquid ^4He was predicted [1]. The weakest binding is to Cs, and indeed non-wetting by liquid ^4He was observed [2]. The wetting temperature, $T_w \approx 2$ K, was measured [3, 4] and it was found that at very low temperature Cs is extremely dry of helium [5]. Film flow measurements of ^4He over Rb also revealed a non-wetting state. Although a wetting temperature could not be measured, it was demonstrated that only a thin 2D-liquid-like film of ^4He forms on Rb below 0.3 K [6].

¹ Author to whom any correspondence should be addressed.

For the system $^4\text{He}\text{--Cs}$ the contact angle, Θ , was measured. Different methods of preparing the Cs have shown, however, different values of Θ [4, 7, 8]. The receding contact angle is in many cases found to be zero, showing that the contact line is strongly pinned, and the advancing contact line can move by thermal activation across pinning sites. These behaviours have been ascribed to various degrees of roughness of the Cs surface. Some experiments, however, have shown a finite receding contact angle [4, 9, 10]. Although there has been no actual measurement of the roughness due to the considerable technical difficulties of examining the surface without contaminating it, it is widely accepted that quench-condensing Cs vapour onto cold substrates gives a rough surface. When these Cs films are annealed, the pinning is slightly reduced [11]. It is thought that the surfaces of bulk Cs and of thermally grown Cs film on tungsten are smoother than the quench-condensed ones [9, 12, 13].

Besides the extreme hysteresis of the movement of the contact line on rough Cs surfaces, there is a memory effect. If such a Cs surface is partially flooded with liquid helium and then fully drained, so that it apparently has no helium film left on it, when it is flooded again the liquid readily flows out to the original boundary between the dry and covered region, but it needs to be forced to go beyond this boundary [14]. The Cs surface has a memory of where it was flooded. A similar effect is seen with sliding helium drops on inclined Cs surfaces [10]. This memory effect can be explained by the ability of micropuddles of liquid ^4He to exist on Cs in thermodynamic equilibrium [15].

From the measured contact angles the determined temperature dependences of the interface free energies $\Delta\sigma(T)$, using Young's law $\Delta\sigma = \sigma_{sv} - \sigma_{sl} = \sigma_{lv} \cos \Theta(T)$, also showed discrepancies. Here σ is the surface free energy and s, l, and v denotes solid, liquid, and vapour. Usually measurements on quench-condensed Cs surfaces did show little temperature dependence, although there are some exceptions. Strong dependence of $\Delta\sigma$ on temperature is observed on Cs prepared from its liquid state [4]. Again, this analysis points to the strong influence of the substrate roughness. From some measurements a new type of interface excitations was detected, namely interface ripples [9, 16], which were indeed recently predicted for the $^4\text{He}\text{--Cs}$ system [17]. In addition, experiments with dilute mixtures of $^3\text{He}/^4\text{He}$ on the same Cs surface revealed both the presence of ^3He interface states and interface ripples [18]. From those experiments a good agreement with theory [19] was obtained and the characteristic parameters, effective mass and bound state energy, of the ^3He interface states could be determined [20].

We have studied the stability of contact lines, separating a metastable ^4He film on Cs from a dry Cs area. This is shown in section 4, after a short description of the experimental set-up in section 2 and the sample preparation in section 3. Below T_w the wet state is metastable with respect to the non-wet state [21]. Furthermore, we investigated dewetting ^4He films on several Cs substrates. On most surfaces a high stability of the contact line (CL) was found and hence no drying of the Cs. Some Cs surfaces, however, showed exceptions to this rule: (a) we observed spontaneous drying with fixed CL and (b) dewetting by receding CL. In one earlier experiment we observed that the metastable ^4He film did suddenly disappear while cooling the Cs substrate far below T_w [22]. Unfortunately, at this time, we could not resolve the dewetting process. In section 5 we have investigated the non-wetting 'thin-film' state of ^4He on Cs using the photoelectron tunnelling technique. With this method we can measure such a film with very high resolution. From very unsaturated vapour pressure conditions towards saturation we find a growth of ^4He on Cs following a 2D-gas law, until a thickness of about one monolayer is reached. Then this growth stops and only very close to liquid–vapour coexistence does the adsorbed helium layer rapidly increase to a few monolayers (2D-liquid-like); the Cs still remains in the non-wet state. These observations are discussed in detail.

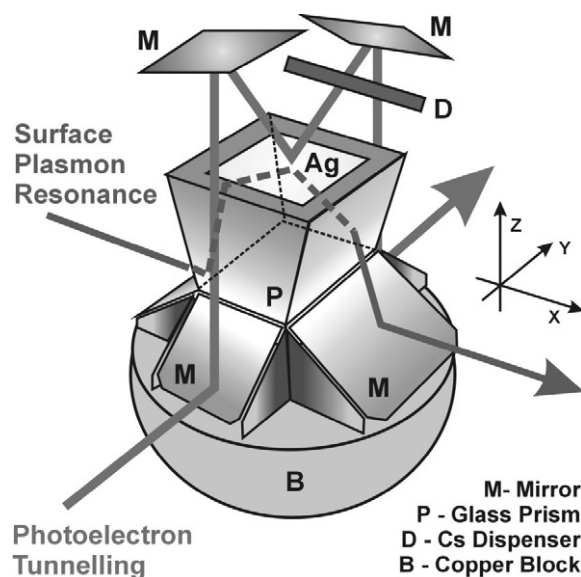


Figure 1. Schematic of the experimental set-up. Both surface plasmon spectroscopy and microscopy are on the x -direction, and the photoelectron tunnelling technique is on the y -direction. For details see [29].

2. Experimental set-up

The core of the experimental set-up (which consists of a thin Ag film deposited onto a BK 7 glass prism) is placed inside a measuring cell, mounted into a ^4He bath cryostat, and probed from outside through optical windows which are symmetrically placed in a four-fold geometry. In this way, we can simultaneously use two complementary techniques; see figure 1. To measure the helium film thickness we use the surface plasmon resonance technique (on the x direction in figure 1) in a Kretschmann configuration. To measure the film thickness locally the surface plasmon spectroscopy (SPS) method is applied. The light beam coming from a laser diode is resonantly coupled into surface plasmons at a certain incidence angle and focused on a photodiode placed outside of the cryostat. When a helium film is adsorbed this causes a resonance detuning. Measuring the shift of the resonance allows us to determine the average thickness of the ^4He film adsorbed on the surface with an accuracy of about 1 \AA .

To monitor the dewetting of deposited ^4He drops and the dynamics of metastable ^4He films we used, in addition, a surface plasmon microscope (SPM). Hereby the sample is illuminated with an expanded light source and the reflected light at a constant resonance angle is imaged on a CCD camera. This allows us to capture images of the whole cesiated surface, and to study the dynamics of wetting. The sensitivity in film thickness of SPM is lower than SPS, but the former leads to a high spatial resolution, the temporal resolution being limited only by the auxiliary recording devices.

To characterize and better understand the behaviour of the system at the early stage of adsorption, the complementary technique of photoelectron tunnelling was introduced and developed. The light which comes from a monochromatic source goes through the optical windows of the cryostat and cell (not shown), is deflected by two mirrors, M, mounted inside the cell, and hits the surface. The Ag layer previously deposited on the glass prism (see section 3) and an electrode (kept at a positive potential) located above the prism are connected

to an electrometer, which measures the photoelectrons leaving the surface and, if a helium film is present, those electrons which tunnel through this film. Outside the cell, an achromatic lens (not shown), which can be positioned via xy stepping motors, focuses the light onto the surface. In this way the whole area can be scanned. A CCD camera which is mounted opposite to the entrance window allows us to check the position and focus of the light spot on the surface.

3. Sample preparation

Even though the glass prism was 'pre-cleaned' it was necessary to perform a rigorous cleaning before mounting in a vapour deposition system. The Ag layer was deposited by thermal evaporation in a vacuum coating system, while monitoring the layer thickness. The pressure inside the evaporator was less than 10^{-6} mbar, at a constant evaporation rate of 1.5 \AA s^{-1} . After reaching the final Ag thickness of 38 nm, the prism was left to thermalize inside the evaporator. Then the Ag/glass prism was horizontally mounted in the experimental cell. We experienced that the pure Ag film severely degrades over a short period of time (≈ 20 h), which has a crucial influence on the coupling of the surface plasmon (SP) resonance. For this reason, we thoroughly pumped out the cell (with a turbo-pump) in order to prevent the air from contaminating the freshly deposited Ag substrate. Meanwhile, the cell was cooled down to about 4 K.

For the *in situ* preparation of the Cs substrate, onto the Ag film, we used the quench-condensation method as follows. The Cs dispenser was slightly heated up while the cell (kept at 4 K) was continuously pumped out in order to remove the impurities desorbed from the dispenser. By opening the shutter mounted in front of the Cs dispenser we started the Cs deposition. The film thickness was monitored by measuring the shift of the SP resonance while evaporating Cs. When the desired Cs film thickness was reached, we closed the shutter and decreased the heating current.

Using a collimation arrangement the evaporated rectangular area of the Cs is smaller than the Ag surface. In this way we always have a wet boundary of known size. Above the Cs there is a small capillary through which helium drops are deposited onto the surface. A second capillary is connected to the bottom of the cell.

4. Wetting dynamics on quench-condensed Cs

At the beginning of the experiments we add helium through the bottom capillary until saturated vapour pressure conditions are ensured. During this process the Cs surface remains dry of helium. After the first deposition of a helium drop through the top capillary, bulk helium covers part of the Cs, forming a sharp contact line. The liquid helium, out of the deposited ^4He drops, rapidly drains towards the wetted Ag boundary, leaving a thin film of about 10 nm thickness. This film is very stable and can only be removed, for example, by laser heating [22].

The CL separates a dry Cs area from the Cs area which is permanently covered with the metastable superfluid film. When further drops, of similar size as the initial one, are deposited on this Cs part then the CL does not move, and after draining of the bulk helium the same metastable film is left [23]. However, if a bigger drop is deposited then a larger area on the Cs is covered, forming a new CL. After a few seconds again a metastable film is left up to this new CL. These observations indicate that the Cs surface is very rough with many pinning centres. This is also seen by the strong fraying of the contact lines.

However, on a few Cs surfaces the metastable helium film disappeared, i.e., there is a spontaneous drying of the Cs. This is illustrated in figure 2. We have analysed the film

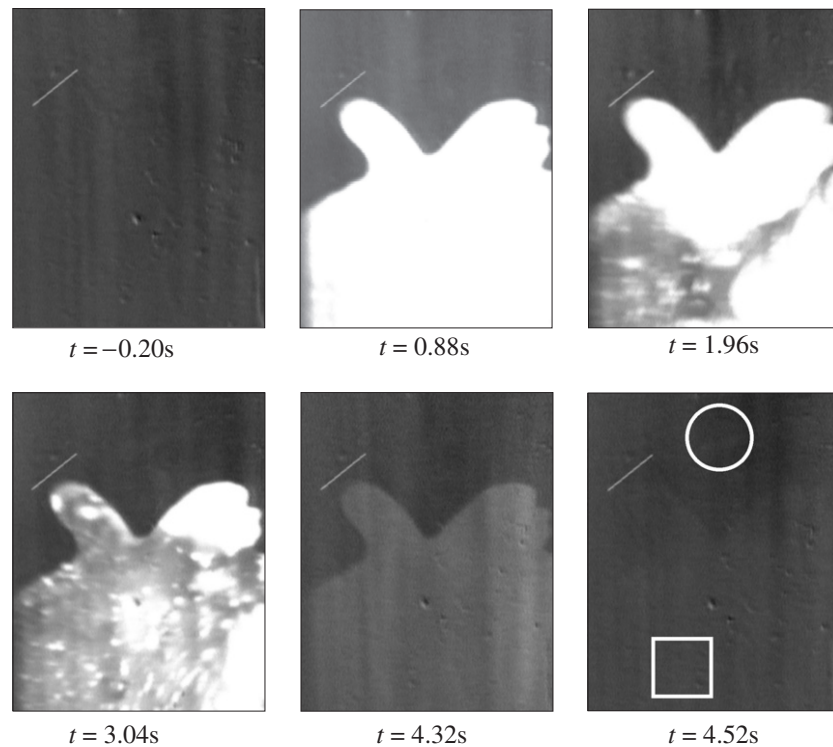


Figure 2. Dewetting of a ^4He drop deposited on a horizontal Cs surface at $T \approx 1.55$ K, shown via a surface plasmon microscope. After about 4.5 s there is hardly any helium visible on the Cs, and after 5 s the surface appears completely dry, similar to the upper area which has not seen bulk helium (i.e., this part of Cs always remains dry). Each image is about $4 \text{ mm} \times 5 \text{ mm}$.

thickness during such a process both on the dry Cs part and the one which is flooded by helium. After about 5 s the thickness of the helium film (determined by the measured reflected light intensity) dropped to zero, indicating a drying of the initially wetted Cs part; see figure 3. We have to note that with the SPM method we can only resolve down to the last 5 monolayers, so any thinner helium film on the Cs would not be detected.

Why spontaneous drying is possible without a receding of the CL remains a question. We assume that the metastable film can evaporate at sharp pinning peaks (where the helium film is very thin) which act as nucleation points. This result points to the important role of the substrate roughness. Roughness has not only consequences for the stability of metastable films but also on contact angle measurements using advancing and receding contact lines [13, 24]. For a strongly pinned CL the receding contact angle will be zero; this is not so for moving contact lines where finite receding contact angles are measured [24]. In contrast, smoother surfaces should show little pinning and small hysteresis in contact angles, as found for Cs surfaces produced from the liquid state (where the surface tension of a thin liquid Cs film should allow for a smoother thin solid Cs substrate) [4, 9].

On a few Cs surfaces we observed, at temperatures slightly below T_w , that the CL can recede. After complete flooding of the Cs surface and draining of the bulk liquid only the metastable helium film is left. The film then recedes in jumps where the CL changes its form, as shown in figure 4. This shows that the receding contact angle is finite. The varying form of the CL can be understood on the basis of randomly distributed pinning centres. Some of these

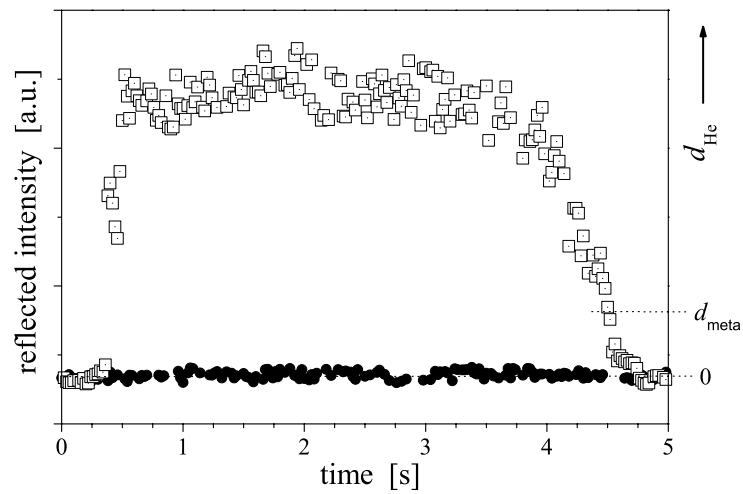


Figure 3. Reflected intensity versus time of the film sequence shown in figure 2. The squares correspond to the Cs area flooded with helium, the circles to the dry Cs part. After about 5 s the initially flooded Cs area is dry again, indicating a spontaneous dewetting. Here $d_{\text{meta}} \approx 10$ nm indicates the thickness of the metastable ^4He film.

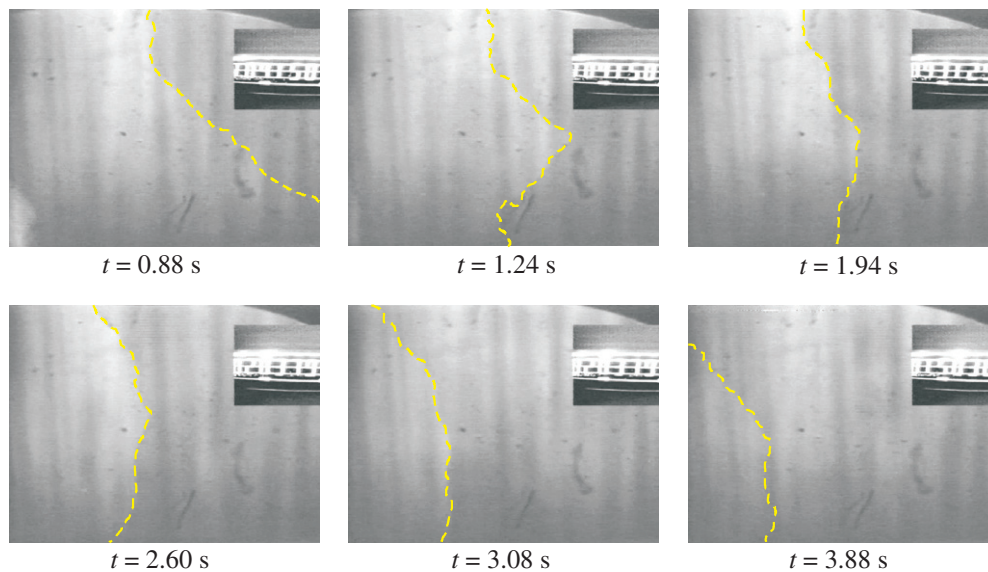


Figure 4. Depinning of a metastable ^4He film on a horizontal Cs surface, at $T \approx 1.65$ K, shown via a surface plasmon microscope. Initially the Cs surface is flooded with a large ^4He drop. The time starts after only the metastable film is left. The CL moves in jumps, i.e., the shown stills indicate each new position of the CL. After about 5 s no helium film is visible anymore, so the Cs surface appears completely dry. In each still a dashed line is drawn to better distinguish between the Cs area with the metastable helium film on and the dry Cs area. Each image is about $5 \text{ mm} \times 4 \text{ mm}$.

(This figure is in colour only in the electronic version)

pinning centres seem to be stronger since they are present in most sequences of the receding CL. The receding CL goes always in the same direction (on the images from right to left). The reason might be a small tilt of our Cs surface, so gravity governs the direction. Another possibility would be a gradient in the surface properties of the Cs. In earlier measurements we checked on the chemical state and homogeneity of our Cs surfaces. However, we did not observe a correlation between variations in work function and pinning centres [22, 23].

Although a rough Cs surface can explain strong pinning, and the presence of random pinning centres causing the random form of the CL, it cannot explain why depinning is observed at higher temperatures, close to T_w (from ≈ 0.3 K below T_w onwards). A possible explanation could be a thermal activation process, as observed on structured Cs surfaces [13, 25]. However, we observe a more sudden onset of depinning as we increase the temperature towards T_w . Once depinning has set in, there is no temperature dependence to be seen, i.e., the velocity of the receding CL does not increase with temperature. We have also checked the stability of the CL at lower temperatures (where no depinning is observed). Here the CL is absolutely stable for more than 30 min (the maximum time measured in our experiments). An explanation of this sudden onset of depinning might be the formation of a thicker non-wetting film, i.e., after a transition from a 2D-gas to a 2D-liquid. Such a thin liquid film may lower the pinning force and so enhance the movement of the CL. If the Cs surface is less rough the transition may happen suddenly once the surface density of the 'thin-film' state has reached a critical value. A transition in 2D was indicated by other experiments [27, 28], and is discussed in more detail in the next section. Again these observation underline the role of the surface roughness and the need for simultaneous wetting studies and surface characterization.

5. The non-wetting 'thin-film'

In order to investigate the adsorption of helium on cesiated surfaces under non-wetting conditions we used the newly developed photoelectron tunnelling method. We start condensing in helium gas and simultaneously illuminate the surface with monochromatic light of a certain wavelength. The incident photons are converted into electrons by the photoelectric effect and—under the applied electric field—leave the surface. If a helium film is adsorbed on the surface the electrons could leave the surface only by tunnelling through the potential barrier, given by the film. So if, for some reasons, the film gets thicker, than fewer and fewer photoelectrons can tunnel, and at a certain thickness no electrons will be able to pass the barrier. This limits the method to detecting only the first few layers of helium (up to about 4 monolayers); however, it is extremely sensitive for measuring very thin films.

Before starting adsorption measurements we first investigated the chemical state of the Cs by measuring the work function. In this case, we performed wavelength scans of the light from 300 to 800 nm. The results have been discussed elsewhere [29]. We concluded that the work function of the Cs is about 1.9 eV, in good agreement with the values found for bulk Cs [30], showing that the films prepared by our evaporation method are rather pure.

Looking in more detail at the energy spectrum of the electrons generated by photoelectric conversion, one can find the energy which is available to the electrons in order to penetrate the potential barrier due to an adsorbed helium film (figure 5). In the low energy part of the spectrum (below 2 eV) one sees that photons can hardly generate photoelectrons, since these energies are very close to the work function of the bare Cs. In the following adsorption experiments we used a photon energy where the photoelectron yield has its maximum (i.e., 2.8 eV).

In the next step, at a constant temperature, we started to slowly condense helium gas into the cell. Measuring the photocurrent emitted from the Cs surface upon irradiation as more

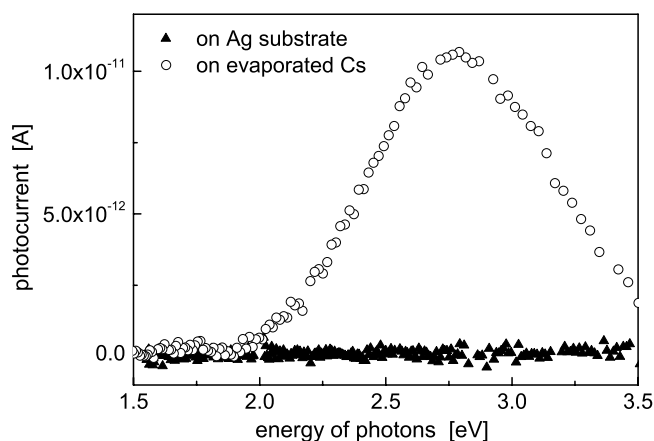


Figure 5. Intensity of the photoelectrons coming from the bare Cs substrate (open symbols). The work function proves the chemical state of the Cs (see the text). Since the work function of Ag is around 4.7 eV, no photoelectrons could be extracted (closed symbols).

and more helium is adsorbed gives information about the helium coverage. For the coverage range above one monolayer, the adsorbed layer can be considered as an additional potential barrier metal surface which should be crossed by the photoelectrons by a tunnelling process. The effective potential barrier of ^4He has a height of about 1 eV [26], and one monolayer of helium is about 0.35 nm. The transmission probability, T_r , of such a barrier of width d is given by $T_r \propto \exp(-2\xi d)$, where ξ represents the decay rate and includes the potential barrier dependence. In this case, one obtains a drop in the transmission coefficient of about one order of magnitude per adsorbed monolayer [31].

All photocurrent curves for adsorption isotherms look qualitatively similar, independent of temperature; see figure 6. At low reduced pressure values, P/P_0 , the photocurrent is decreasing, and then comes a ‘plateau’ region, followed—before reaching saturated vapour pressure—by a subsequent decrease.

Away from the liquid–vapour coexistence the helium coverage is expected to be very low, such that photoelectrons can easily leave the Cs surface. The contribution to the photocurrent becomes smaller after the first few monolayers have been completed, because then the electrons can only tunnel through the helium barrier. At the beginning of each adsorption isotherm (i.e., when helium gas is first added to the cell), we start with a maximum photocurrent value. We observe that the higher the temperature, the higher is the initial value of the photocurrent (see figure 6). This is due to the fact that, in order to carry out a new photocurrent measurement at a different temperature, we first had to pump out the helium. However, due to the finite pumping speed of our turbo-pump the last fraction of helium can be better removed at higher temperature (due to the higher vapour pressure).

Far off liquid–vapour coexistence the decay in photocurrent, of about one order of magnitude, gets steeper with temperature. Then, although continuously condensing in helium gas, the photocurrent decreases only very slowly over a long relative pressure range; see figure 6. This ‘plateau’ in photocurrent becomes broader at higher temperature. These features could be observed on all measurements we have done over the temperature range 1.3–2 K. The ‘plateau’ happens at slightly different values, but the general behaviour is independent of speed of condensation, and is reversible if helium is pumped out. In this context, we conclude that the beginning of the ‘plateau’ corresponds to the formation of the first helium layer and the

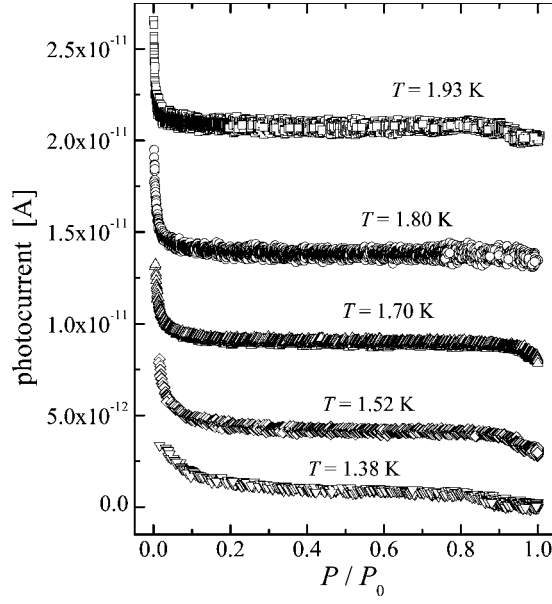


Figure 6. Series of measurements at different temperatures of the photoelectrons which tunnel through an adsorbed helium film on a quench-condensed Cs surface (see the text for details). For the sake of clarity the curves are shifted to the $T = 1.38$ K curve by 3, 8, 13, and 20 pA, respectively.

thickness of this adsorbed layer remains nearly constant up to the end of the 'plateau'. Only close to saturated vapour pressure conditions does the photocurrent decrease further.

In the submonolayer regime of helium coverage there is little knowledge about the governing adsorption mechanism, and the possible change of the Cs work function due to the presence of He should be taken into account. The adsorbed helium atoms on the Cs surface still tend to reduce the photocurrent and are expected to behave like a 2D-gas. The grand potential of a classical noninteracting ideal gas in 2D is given by

$$\Phi = -k_B T \exp\left(\frac{\mu - \epsilon_1}{k_B T}\right) \int_0^\infty n(k) dk \exp\left(\frac{-\hbar^2 k^2}{2mk_B T}\right) \quad (1)$$

where ϵ_1 is the binding energy of a single helium atom to the Cs ($\epsilon_1/k_B \approx 3$ K), m is the mass of a ^4He atom and $n(k)$ is the density of particle states in k space for the 2D system of area A . Evaluating the integral in equation (1) gives the grand potential as [27]

$$\Phi = -\frac{Am}{2\pi} \left(\frac{k_B T}{\hbar}\right)^2 \exp\left(\frac{\mu - \epsilon_1}{k_B T}\right). \quad (2)$$

Using equation (2), the surface coverage, per unit area, is calculated as

$$n_{2D\text{-gas}} = -\frac{1}{A} \left(\frac{d\Phi}{d\mu}\right)_{A,T} \propto T \exp\left(\frac{\mu - \epsilon_1}{k_B T}\right). \quad (3)$$

From the data in figure 7 one can observe that far away from coexistence the system behaves as a 2D-gas and the data follow an exponential dependence. The slope of the linear part of the curves changes with the temperature at which the adsorption takes place. As the temperature decreases the slope becomes steeper, as one would expect from the temperature dependence of a 2D-gas, equation (3).

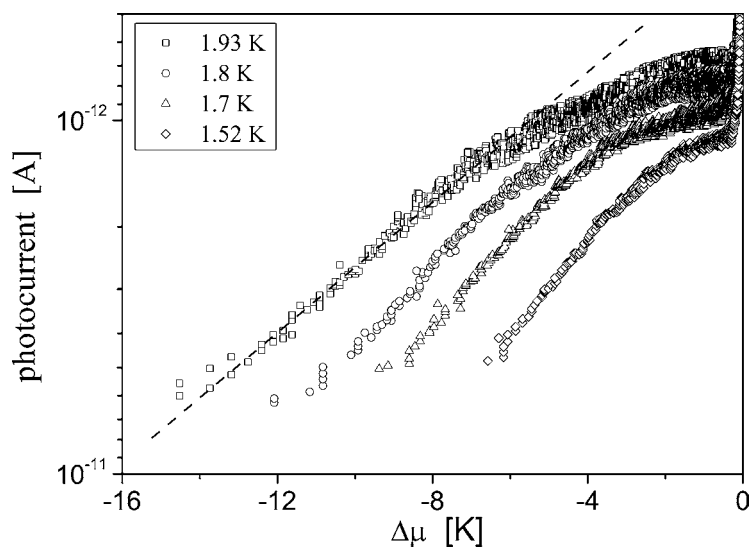


Figure 7. The dependence of the photocurrent focusing on the region far away from coexistence. The photocurrent drops by about one order of magnitude exponentially with chemical potential. This indicates the growth of a thin helium film following a 2D-gas law. Then the current remain nearly constant (with a thickness of about one monolayer) and only very close to coexistence drops further (see figure 8 for more details).

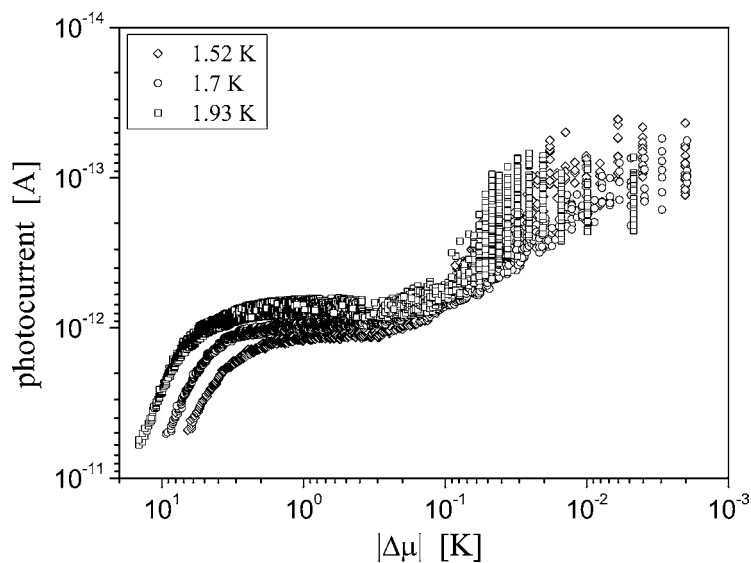


Figure 8. The dependence of the photocurrent close to coexistence. When the photocurrent levels off at coexistence there are 2–3 monolayers of ^4He on the quench-condensed Cs surface.

As the system approaches coexistence (i.e., $P \rightarrow P_0$) another drop in photocurrent of nearly two orders of magnitude is found; see figure 8. This we interpret—in terms of coverage—as the transition from one monolayer to a second (or perhaps even third) helium layer, which acts like an additional potential barrier which should be passed by the photoelectrons. One should note that the value of the photocurrent is still finite at $P = P_0$,

i.e., $\Delta\mu = 0$, although it goes close to the noise level of measuring photocurrent. So the system is still in the non-wet state. The helium thickness in that region does not depend on temperature. We assume that at liquid–vapour coexistence a 2D-liquid has formed as the thermodynamic stable non-wetting film on the Cs surface [27, 28].

6. Conclusions

We have observed, on the one hand, strong pinning of contact lines on most Cs surfaces and, on the other hand, receding contact lines on a few Cs surfaces. The pinned contact lines appeared stable, since we could not detect any movement at all. We saw an advancing of the CL when bulk liquid causes a flooding of a bigger area on the Cs. After such an event a new, again stable, CL is seen. On some Cs surfaces we detected spontaneous drying of the Cs surface, i.e., the metastable helium film disappeared. However, during this drying process the CL did not recede. This is in contrast to a few Cs surfaces where depinning of the CL is seen. Such a scenario, however, only happened for temperatures close to T_w . A possible interpretation of the temperature dependence is the formation of a non-wetting 2D-liquid film, which may enhance the receding. The overall conclusion of these investigations is the need for surface characterization when discussing wetting parameters and hysteresis effects in moving CLs. Such investigations have to be done simultaneously with the wetting studies so that correlations can be drawn. For this reason we have established a new set-up which allows such experiments: via a surface tunnelling microscope, with large scanning facility and working at low temperature, we can characterize our *in situ* prepared Cs samples on the microscopic scale over a large area, and via the surface plasmon techniques we can monitor the dynamics and measure the thickness of helium films not wetting such surfaces. First success in imaging Cs deposited on HOPG and mica with this set-up has been demonstrated [32].

Furthermore, we have shown that the photoelectron tunnelling technique can resolve thin helium films adsorbed on a quench-condensed Cs surface with high accuracy, and can be used to investigate the features of the non-wetting state. We found that far from coexistence the system is dilute with a helium coverage below one monolayer. Close to coexistence a growth of a few monolayers is observed, but the surface is still in the non-wet state.

Acknowledgment

This work was supported by the DFG-Schwerpunkt 'Wetting and Structure Formation at Interfaces' under Kl 1186/1.

References

- [1] Cheng E, Cole M W, Saam W F and Treiner J 1991 *Phys. Rev. Lett.* **67** 1007
- [2] Nacher P J and Dupont-Roc J 1991 *Phys. Rev. Lett.* **67** 2966
- [3] Rutledge J E and Taborek P 1992 *Phys. Rev. Lett.* **69** 937
- [4] Klier J, Stefanyi P and Wyatt A F G 1995 *Phys. Rev. Lett.* **75** 3709
- [5] Stefanyi P, Klier J and Wyatt A F G 1994 *Phys. Rev. Lett.* **73** 692
- [6] Klier J and Wyatt A F G 2002 *Phys. Rev. B* **65** 212504
- [7] Ross D, Rutledge J E and Taborek P 1997 *Science* **278** 664
- [8] Rolley E and Guthmann C 1997 *J. Low Temp. Phys.* **108** 1
- [9] Klier J and Wyatt A F G 1998 *J. Low Temp. Phys.* **110** 919
- [10] Rutledge J E, Ross D and Taborek P 1998 *J. Low Temp. Phys.* **113** 811
- [11] Ross D, Taborek P and Rutledge J E 1998 *J. Low Temp. Phys.* **111** 1
- [12] Klier J and Wyatt A F G 2000 *Physica B* **280** 85

-
- [13] Prevost A, Poujade M, Rolley E and Guthmann C 2000 *Physica B* **280** 80
 - [14] Herminghaus S, Vorberg J, Gau H, Conradt R, Reinelt D, Ulmer H, Leiderer P and Przyrembel M 1997 *Ann. Phys., Lpz.* **6** 425
 - [15] Wyatt A F G and Klier J 2000 *Phys. Rev. Lett.* **85** 2769
Wyatt A F G and Klier J 2001 *Phys. Rev. Lett.* **87** 279602
 - [16] Klier J and Wyatt A F G 1996 *Czech. J. Phys.* **46** 439
 - [17] Clements B E, Krotscheck E and Tymczak C J 1997 *J. Low Temp. Phys.* **107** 387
 - [18] Klier J and Wyatt A F G 1996 *Phys. Rev. B* **54** 7350
 - [19] Bashkin E, Pavloff N and Treiner J 1995 *J. Low Temp. Phys.* **99** 659
 - [20] Klier J and Wyatt A F G 1999 *J. Low Temp. Phys.* **116** 61
 - [21] Bonn D and Indekeu J O 1995 *Phys. Rev. Lett.* **74** 3844
 - [22] Reinelt D, Klier J and Leiderer P 1998 *J. Low Temp. Phys.* **113** 805
 - [23] Reinelt D, Engel A and Klier J 2000 *Physica B* **284** 149
 - [24] Phillips J A, Taborek P and Rutledge J E 1998 *J. Low Temp. Phys.* **113** 829
 - [25] Prevost A, Rolley E and Guthmann C 1999 *Phys. Rev. Lett.* **83** 348
 - [26] Woolf M A and Rayfield G W 1965 *Phys. Rev. Lett.* **15** 235
 - [27] Klier J and Wyatt A F G 1998 *J. Low Temp. Phys.* **113** 817
 - [28] Iov V, Klier J and Leiderer P 2003 *Physica B* **329** 242
 - [29] Iov V, Klier J and Leiderer P 2002 *J. Low Temp. Phys.* **126** 367
 - [30] Gregory P E, Chye P, Sunami H and Spicer W E 1975 *J. Appl. Phys.* **46** 3525
 - [31] Conradt R, Przyrembel M, Herminghaus S and Leiderer P 1996 *Czech. J. Phys.* **46** 445
 - [32] Zech M, Fubel A, Leiderer P and Klier J 2004 *J. Low Temp. Phys.* **137** 179